Published in final edited form as:
Neuron. 2011 February 24; 69(4): 721–735. doi:10.1016/j.neuron.2011.01.014.

Mir-17-3p Controls Spinal Neural Progenitor Patterning by Regulating Olig2/Irx3 Cross-repressive Loop

Jun-An Chen[1], **Yuan-Ping Huang**[1], **Esteban O. Mazzoni**[1], **G. Christopher Tan**[1], **Jiri Zavadil**[2], and **Hynek Wichterle**[1,*]

[1] Departments of Pathology and Cell Biology, Neurology, and Neuroscience, Center for Motor Neuron Biology and Disease, Columbia University Medical Center, New York, NY, USA

[2] Department of Pathology, NYU Cancer Institute and Center for Health Informatics and Bioinformatics, New York University Langone Medical Center, New York, NY 10016, USA

SUMMARY

Neural patterning relies on transcriptional cross-repressive interactions that ensure unequivocal assignment of neural progenitor identity to proliferating cells. Progenitors of spinal motor neurons (pMN) and V2 interneurons (p2) are specified by a pair of cross-repressive transcription factors Olig2 and Irx3. Lineage tracing revealed that many p2 progenitors transiently express the pMN marker Olig2 during spinal cord development. Here we demonstrate that the repression of Olig2 in p2 domain is controlled by *mir-17-3p* microRNA-mediated silencing of *Olig2* mRNA. Mice lacking all microRNAs or just the *mir-17~92* cluster manifest a dorsal shift in pMN/p2 boundary and impairment in the production of V2 interneurons. Our findings suggest that microRNA-mediated repression of *Olig2* mRNA plays a critical role during the patterning of ventral spinal progenitor domains by shifting the balance of cross-repressive interactions between Olig2 and Irx3 transcription factors.

Keywords

microRNA; embryonic stem cells; Olig2; Irx3; mir-17~92; motor neurons; neural patterning; interneuron; spinal cord; bistable loop; progenitor domain; spatial patterning; minor strand miRNA; regulatory network

INTRODUCTION

Specification of diverse neuronal cell types during development depends on subdivision of nascent neuroepithelium into discrete progenitor domains by transient patterning signals. The assignment of unambiguous progenitor identity to neural cells relies on genetic switches that are often based on pairs of transcriptional cross-repressors (Briscoe et al., 2000; Dessaud et al., 2008; Jessell, 2000). Development of the spinal cord is particularly well elucidated in this respect. Dorso-ventral patterning of the nascent ventral neural tube is controlled by Sonic hedgehog (Shh) protein emanating from the notochord and floor plate and a more diffuse retinoid signal synthesized by paraxial mesoderm (Briscoe et al., 2000;

Correspondence: H. Wichterle, (phone): 212 342 3928, (fax): 212 342 1555, hw350@columbia.edu.

Briscoe et al., 1999; Novitch et al., 2003). Pairs of cross-repressive transcription factors, whose expression is differentially sensitive to the patterning signals establish five discrete ventral spinal progenitor domains (Figure 1A). Specifically, the motor neuron progenitor (pMN) marker Olig2 is engaged in a cross-repressive interaction with Irx3 to define the dorsal boundary of the pMN domain (Chen et al., 2007; Novitch et al., 2001; Zhou and Anderson, 2002). The ventral Olig2 boundary is established by the repressive activity of Nkx2.2 transcription factor expressed in the p3 progenitor domain (Briscoe et al., 2000; Briscoe et al., 1999).

Interestingly, lineage tracing experiments in which *Cre* recombinase was knocked into domain specific patterning genes *Olig1*, *Olig2* or *Dbx1* (Dessaud et al., 2010; Dessaud et al., 2007; Wu et al., 2006) revealed that each of these factors is transiently expressed in a broad ventral spinal region spanning three or more neighboring progenitor domains. Thus, the state of cross-repressive loops has to be malleable, and the initial broad expression of domain specific determinants needs to be refined during development. Repression of Olig2 in non-motor neuron progenitors appears to be in part achieved by a temporal adaptation of spinal cells to Shh signal. Clearance of Olig2 from the p3 domain depends on the induction of a repressor Nkx2.2 in response to a sustained Shh signaling while more passive loss of Olig2 expression in p2 domain is proposed to be due to a developmental de-sensitization of progenitors to the Shh signal (Dessaud et al., 2010; Dessaud et al., 2007).

Here we considered whether repression of Olig2 within p2 progenitor domain might rely on additional regulatory mechanisms. Specifically, we examined whether microRNAs (miRNAs), small non-coding RNAs generated by the cytoplasmic RNaseIII enzyme Dicer, might contribute to cross-repressive interactions at progenitor boundaries via their ability to silence translation of target mRNAs. miRNAs play a critical role in the specification of postmitotic neuronal identity in *C. elegans*, where miRNAs *lsy-6* and *mir-273* are integral parts of a bistable loop controlling the left and right subtype identities of ASE chemosensory neurons (Chang et al., 2004; Johnston et al., 2005), and in the specification of neural vs. non-neural identity in Drosophila peripheral nervous system (Li et al., 2006). To what extent miRNAs are involved in the segregation of neuronal subtypes in vertebrates remains unclear. The analysis of neural specific *Dicer* mutants in mammals established miRNA roles in the control of temporal transitions from early to late neural progenitors (Georgi and Reh, 2010) or from progenitors to postmitotic neurons (Fineberg et al., 2009). A role for miRNAs in spatial patterning has been demonstrated in the developing mesoderm where knockdown of *mir-196* results in an expansion of Hoxb8 expression and homeotic transformation of axial skeleton (Mansfield et al., 2004; McGlinn et al., 2009). In contrast, whether miRNAs are involved in spatial patterning of neural progenitors is not well established (Fineberg et al., 2009). This might be in part due to the lack of a simple genetic system to probe miRNA function during the early stages of mammalian development when progenitor identity is specified. A complete loss of Dicer function in mice leads to embryonic lethality before neural tissue formation (Bernstein et al., 2003) and selective disruption of Dicer function in early neural progenitors is complicated by the lack of suitable drivers expressed in prospective neural tissue and by the relative stability of existing miRNAs (Davis et al., 2008).

Here we examined miRNA function by employing an embryonic stem (ES) cell differentiation system that faithfully recapitulates patterning of the developing spinal cord (Wichterle et al., 2002). By disrupting miRNA biogenesis during simulated dorso-ventral patterning of differentiating ES cells we observed a conversion of Olig2 negative V2 interneuron progenitors (p2) to Olig2 positive motor neuron progenitors (pMN). We determined that *mir-17-3p*, a member of the *mir-17~92* cluster (He et al., 2005; Ventura et al., 2008), is required for silencing of transient Olig2 expression in p2 progenitors, both *in*

vitro and *in vivo*. Thus, miRNA-mediated regulation of transcriptional programs might play a more general role in the refinement and positioning of spatial boundaries in the developing neural tissue.

RESULTS

pMN Marker Olig2 is Transiently Expressed by p2 Progenitors

Developing spinal progenitors undergo a progressive adjustment in the expression profile of patterning transcription factors to refine the position and size of individual progenitor domains (Figure 1A) (Dessaud et al., 2010; Dessaud et al., 2007). To identify all spinal neural cells that descend from Olig2 expressing progenitors we performed a lineage tracing experiment using *Olig2*$^{Cre/+}$ mice in which one allele of *Olig2* is replaced with a gene coding *Cre* recombinase (Figure 1B) (Dessaud et al., 2010; Dessaud et al., 2007). Analysis of *Olig2*$^{Cre/+}$*; ROSA26-loxp-STOP-loxp-YFP* embryos on day 11.5 of development (E11.5) demonstrated that *Cre* is transiently expressed not only by pMN progenitors, but also by p3 and a significant subset of p2 progenitors (Figures 1C–1H and Figure S1) (Dessaud et al., 2010; Dessaud et al., 2007). Dorsal to the pMN domain YFP expression was detected in ~40% of Irx3^{on}, Nkx6.1^{on}, Olig2^{off} p2 progenitors, ~40% postmitotic Chx10^{on} V2a and ~20% Gata3^{on} V2b interneurons (Figures 1C–1J and Figure S1). Occasionally we observed isolated YFP^{on} clones within more dorsal progenitor domains (Figure 1H), but a majority of postmitotic V0 and V1 interneurons expressing Evx1 and En1 were YFP^{off} (Figures S1B and S1C). Together, these results provide genetic evidence that *Olig2* is transiently expressed by a subset of p2 progenitors during spinal cord development and that its expression is subsequently repressed to achieve Olig2^{off}, Irx3^{on} transcriptional state compatible with p2 progenitor identity (Figure 1K).

Dorsal Expansion of Olig2 Expression in the Absence of Dicer Function

Requirement for a rapid and efficient repression of Olig2 prompted us to examine whether miRNA-mediated silencing might be involved in the process of ventral spinal cord patterning. To circumvent the early embryonic lethality of mice in which miRNA biogenesis is blocked (Bernstein et al., 2003), we examined miRNA function in an *in vitro* embryonic stem (ES) cell differentiation system recapitulating ventral spinal cord patterning in response to variable concentration of Sonic Hedgehog agonist (SAG) (Wichterle et al., 2002). ES cells lacking functional Dicer enzyme are unstable and exhibit propensity to accumulate chromosomal defects (Kanellopoulou et al., 2005). Therefore we derived a *CAGG-CreER*$^{+/-}$; *Dicer*$^{loxp/loxp}$ ES cell line (*Dicer*$^{f/f}$) in which both *Dicer* alleles can be disrupted by 4-Hydroxytamoxifen (4OH-TM) treatment (Figure 2A and Figure S2A) (Harfe et al., 2005; Hayashi and McMahon, 2002). Treatment of *Dicer*$^{f/f}$ ES cells with 4OH-TM leads to efficient recombination of both *Dicer* alleles (producing *Dicer*$^{-/-}$ cells) (Figure S2B) accompanied by a ~10 fold decrease in the level of a ubiquitously expressed miRNA *mir-16* on day 3 of differentiation when cells are acquiring dorso-ventral progenitor identity (Figure S2C).

To examine whether decreased levels of miRNAs affect dorso-ventral spinal progenitor patterning, differentiating 4OH-TM treated control and conditional *Dicer*$^{-/-}$ ES cells were exposed to low (lo[Hh], 5~10nM) and high (hi[Hh], 500nM) concentration of SAG on day 2 of differentiation (Figure 2A). Two days later on day 4 of differentiation, control cells exposed to lo[Hh] acquired preferentially p0/p1 interneuron progenitor identity (Irx3^{on}, Nkx6.1^{off}, Pax7^{off}) while a smaller fraction of cells adopted p2 identity (Irx3^{on}, Nkx6.1^{on}, Olig2^{off}) (Figures 2B and 2D). Identical treatment of the *Dicer*$^{-/-}$ ES cell line resulted in a significant reduction in the percentage of progenitors expressing p2 markers that was accompanied by a corresponding increase in the percentage of Irx3^{off}, Nkx6.1^{on}, Olig2^{on}

MN progenitors (n = 3 independent experiments, Figure 2F), indicative of a conversion of p2 to pMN identity in the absence of miRNAs. To determine whether specification of other ventral progenitor domains is affected in the *Dicer*$^{-/-}$ cells we examined expression of progenitor markers in ES cells differentiated under hi[Hh] conditions. In contrast to lo[Hh] condition, we did not detect overt defects in neural progenitor patterning. Comparable percentages of Olig2 expressing pMN progenitors, and Nkx2.2 expressing p3 interneuron progenitors were detected in the control and *Dicer*$^{-/-}$ ES cell lines on day 4 of differentiation (Figures 2G–2K). These results indicate that under the examined differentiation conditions, Dicer activity is specifically required for the efficient specification of p2 and suppression of pMN progenitor identity of differentiating ES cells exposed to low concentration of Hh.

Next we examined whether p2/pMN specification *in vivo* also relies on Dicer function. Since *Dicer* mutant mice die on embryonic day 7.5 (E7.5) (Bernstein et al., 2003) we utilized *CAGG-CreER* conditional *Dicer* knockout mice (i.e. *CAGG-CreER*$^{+/-}$; *Dicer*$^{loxp/loxp}$) (Figures S2D and S2E). To ensure effective loss of miRNAs following Dicer deletion, tamoxifen (TM) was injected intraperitoneally into pregnant dams on E5~5.5 to generate *Dicer*$^{-/-}$ embryos and dorso-ventral pattering was assayed four days later on E9.5 (Figure 2L). *Dicer*$^{-/-}$ mice exhibited a shorter body axis and most mutant embryos died by E11.5 (Figures S2F and S2G). The ubiquitously expressed miRNA *mir-16* was effectively depleted in the neural tube of E9.5 knockout mice as determined by *in situ* hybridization using a locked nucleic acid (LNA) probe (Figures S2H andS2 I).

Since the deletion of *Dicer* gene is not limited to neural tissue, we considered whether global depletion of miRNAs might affect specification of signaling centers essential for spinal cord patterning. Ventral expression domain of Shh in the floor plate and notochord, and paraxial mesodermal expression domain of the RA synthesizing enzyme retinaldehyde dehydrogenase-2 (Raldh2) were not affected in E9.5 *Dicer*$^{-/-}$ embryos (Figures S2J and S2K). Despite the normal appearance of the developing spinal cord and adjacent patterning centers, all examined *Dicer*$^{-/-}$ embryos exhibited a dorsal expansion of pMN domain marker Olig2 (n= 5, Figures 2M–2T) compared to their heterozygous or wild type littermates. To investigate the precise position of the dorsal limit of Olig2 expansion in *Dicer*$^{-/-}$ embryos, we quantified p2 progenitors co-expressing Nkx6.1 and Irx3. While the total number of Nkx6.1^{on} cells was not changed in mutant embryos, the number of p2 progenitors (Nkx6.1^{on}, Irx3^{on}) was markedly diminished (Figures 2Q–2R and 2U), suggesting that the Olig2 expression domain expanded at the expense of p2 progenitors. In contrast, the number of Nkx2.2 expressing p3 progenitors was unchanged as was the position of Pax7 expressing dorsal spinal progenitors (Figures2S–2U, and data not shown), suggesting that the dorsal shift of the pMN/p2 progenitor boundary is likely not a consequence of an overall increase in Shh signaling accompanied by a global dorsal shift of all ventral progenitor domain boundaries. Considering that Olig2 is transiently expressed by p2 progenitors during early stages of spinal cord development we propose that the failure to effectively repress its expression in *Dicer*$^{-/-}$ embryos results in a conversion of a subset of p2 progenitors to Olig2 expressing pMN-like cells (Figure 2V).

Reciprocal Expression of *mir-17* and its Predicted Target Olig2 in the Ventral Spinal Cord

The ectopic expression of Olig2 in p2 progenitors in *Dicer*$^{-/-}$ cells and embryos raised the possibility that miRNAs expressed in the p2 domain might be involved in the silencing of Olig2 expression. To identify miRNAs that are enriched in p0~p2 domain we profiled expression of 343 miRNAs in ES cell derived ventral spinal progenitors treated with lo[Hh]or hi[Hh] using the murine TaqMan Low Density Arrays (TLDA) (Figure 3A). TLDA arrays are based on qPCR technology, providing a quantitative assessment of expressed miRNAs. The pairwise comparison of small RNA enriched samples isolated from cells

differentiated under the two conditions identified 53 miRNAs (15.4%) significantly enriched in lo[Hh] progenitors and only 8 miRNAs (2.3%) enriched in hi[Hh] progenitors (Figure 3B). Out of the lo[Hh] enriched miRNAs only two miRNAs, *mir-17-3p* and *mir-302b*, were predicted to target *Olig2* mRNA by miRNA target prediction algorithms (Targetscan 4.2, miRanda, and MicroCosm Targets) (Figure 3C). Independent qPCR analysis (n=3) confirmed ~4.5 fold enrichment of *mir-17-3p* and ~2 fold enrichment of *mir-302b* in lo[Hh] derived p0–p2 progenitors compared to hi[Hh] derived p3-pMN progenitors (Figure 3D). The highly enriched *mir-17-3p* is a passenger strand (also known as *mir-17**) produced from an oncomir cluster *mir-17~92* (He et al., 2005; Ventura et al., 2008). Passenger strand (miRNA*) refers to a strand of miRNA duplex that is less likely to be incorporated into the RISC complex during miRNA biogenesis, yet many passenger strands were recently shown to be utilized in mRNA silencing (Okamura et al., 2008). Interestingly, a closer examination of *mir-17-5p*, the major product of *mir-17*, revealed a striking similarity of its seed sequence to the seed sequence of *mir-302b* (Figure 3E). Thus, both strands of *mir-17* might contribute to Olig2 silencing through binding to *mir-17-3p* and *mir-302b* target sites within *Olig2* 3′UTR (Figure 3E). Based on these observations we elected to further examine the function of *mir-17* during spinal cord patterning.

In situ hybridization and immunohistochemistry on adjacent mouse E9.5 spinal cord sections revealed that *mir-17-3p* was enriched in the dorsal spinal region corresponding to Irx3 expression domain and was reduced in the Olig2 expressing motor neuron progenitor domain (Figures 4A and 4B). To examine whether Olig2 and Irx3 transcription factors might control *mir-17-3p* expression, we generated “Tet-on” inducible Irx3 and Olig2 ES cell lines (Figure 4C) (Ting et al., 2005). Induced expression of Olig2 in progenitors derived under lo[Hh] condition by doxycycline treatment on day 3 of differentiation resulted in an efficient suppression of Irx3 expression (Figures 4D and 4E) and in a decrease in both *mir-17-3p* and *-5p* levels on day 4 (Figure 4H). Conversely, induction of Irx3 in hi[Hh] differentiated progenitors repressed Olig2 expression within the pMN cells (Figures 4F and 4G) and increased *mir-17-5p* and *-3p* expression (Figure 4H). To determine whether Olig2 is necessary for *mir-17* repression, we derived an $Olig2^{-/-}$ ES cell line and differentiated it under condition that normally promotes specification of pMNs. The absence of Olig2 results in a modest increase in Irx3 expression and correspondingly modest increase (~1.5 fold) in *mir-17-3p* and *-5p* expression (n= 3 independent experiments, Figure S3). Together, these observations indicate that Olig2 represses *mir-17* indirectly, likely through the repression of Irx3 or another p2-specific positive regulator of *mir-17* expression.

To examine whether *mir-17* is sufficient to switch the state of the Olig2/Irx3 cross-repressive loop we developed a “Tet-on” inducible ES cell line, in which *mir-17* was inserted into the 3′UTR of an inducible GFP construct (Figure 4I and Figure S4A) (Wang et al., 2007). To faithfully mimic dynamic changes in Shh activity during the patterning of p2 progenitor domain (Dessaud et al., 2010), inducible ES cells were differentiated by a transient exposure of embryoid bodies to an intermediate concentration of SAG (med[Hh]: 100nM) between days 2 and 3 of differentiation. Under this condition we observed that induction of *mir-17* by doxycycline treatment on day 3 resulted in a decrease in the fraction of $Nkx6.1^{on}$ cells expressing Olig2 and a concomitant increase in the fraction of progenitors expressing Irx3 on day 4 of differentiation (Figures 4J and 4K; Figure S4B). These findings indicate that induction of *mir-17* expression is sufficient to effectively switch the state of the patterning cross-repressive loop and to convert progenitors from pMN to p2 identity.

Olig2 is Directly Silenced by *mir-17-3p*

To determine whether *Olig2* is a direct target of *mir-17*, we constructed a luciferase reporter containing the full length 3′ UTR of *Olig2* harboring the predicted *mir-17* target sites (Figure 5A). Co-transfection of the luciferase construct with the *mir-17* expression vector

resulted in a ~50% reduction in luciferase activity in HeLa cells (Figure 5B). The miRNA target prediction algorithms identified two potential binding sites for *mir-17-3p* and two potential binding sites for *mir-302b* with a high degree of homology to the *mir-17-5p* sequence (Figure 3E). To determine which *mir-17* strand is primarily responsible for *Olig2* regulation we mutated the two canonical *mir-17-3p* binding sites (3p-Mut); the two canonical *mir-302b/mir-17-5p* binding sites (5p-Mut); or all four predicted binding sites (3p/5p-Mut) in *Olig2* 3′UTR reporter constructs (Figure 5A). While both 3p-Mut and 3p/5p-Mut constructs were completely insensitive to *mir-17* mediated silencing, the silencing of constructs with mutated putative *mir-17-5p* binding sites was not compromised (Figure 5B). We conclude that *mir-17-3*p binding sites alone are critical for *mir-17* mediated silencing of *Olig2* 3′UTR.

This observation prompted us to examine whether *mir-17-3p* is sufficient to silence Olig2 expression. We developed a “Tet-on” inducible ES cell lines, in which complementary *mir-17-3p* or *mir-17-5p* hairpins flanked by *mir-30* shMir backbone were inserted into the 3′UTR of an inducible GFP construct (Figure 5C) (Stegmeier et al., 2005). To provide internal control, inducible ES cells were spiked with parental ES cells, thus producing mosaic embryoid bodies composed of patches of GFP^{off} control cells and GFP^{on} experimental cells expressing inducible miRNAs upon doxycycline treatment (Figure 5D). ES cells were differentiated under hi[Hh] condition and miRNA expression was induced on day 3 of differentiation, 24 hours prior to the normal onset of Olig2 expression. Induction of *mir-17* (Figure 4I) resulted in a selective repression of Olig2 without affecting Nkx6.1 expression, demonstrating that *mir-17* is able to suppress Olig2 when induced in motor neuron progenitors (Figure 5D). Similarly, induction of *mir-17-3p* effectively silenced Olig2 expression while induction of *mir-17-5p* had no discernible effect on the pattern of Olig2 expression (Figure 5D). Together, these results provide evidence that *mir-17-3p* alone is sufficient to silence Olig2 expression.

mir-17~92$^{-/-}$ Embryos Exhibit Dorsal Expansion of Olig2 Domain and Decrease in V2 Interneurons

To test the requirement for *mir-17* in the patterning of the ventral spinal cord and in the specification of p2 progenitor identity more directly we analyzed *mir-17~92* mutant ES cells and mice. The deletion of the *mir-17~92* cluster in mice results in perinatal lethality and developmental defects in the heart, lungs, and immune system (Ventura et al., 2008). Differentiation of *mir-17~92*$^{-/-}$ ES cell line (Mu et al., 2009; Ventura et al., 2008) (Figures S5A–S5D) under lo[Hh] condition revealed defects in p2 progenitor specification that were reminiscent of the defects observed in *Dicer*$^{-/-}$ cells (Figures 6A–6E and Figures 2B–2F). We observed an increase in the fraction of $Nkx6.1^{on}$ cells expressing Olig2 on day 4 of differentiation, indicative of a fate switch from p2 to pMN identity (Figure 6E). It is unlikely that the *mir-17~92*$^{-/-}$ phenotype is caused by a change in sensitivity of differentiating cells to RA and Hh signals, since expression levels of the key mediators and targets of RA and Shh signaling pathways (*RARα*, *β*, *γ*, and *Gli1*, *2*, *3* and *Ptch1*) were similar in the *mir-17~92*$^{-/-}$ and control cells (Figures S5E and S5F).

To determine whether the loss of the *mir-17~92* cluster results in ventral spinal cord patterning defects *in vivo*, we examined expression of progenitor markers in the neural tube of *mir-17~92*$^{-/-}$ embryos. Consistent with our *in vitro* observations, the Olig2 expression domain expanded dorsally while the number of p2 progenitors decreased ~65%. In contrast, the dorsal boundary of ventral spinal markers Nkx2.2 and Nkx6.1, and ventral boundary of dorsal spinal marker Pax7 was not affected (Figures7A–7I and data not shown) indicating that the loss of this miRNA cluster does not lead to a global deregulation of spinal cord development and patterning. The neural tube patterning phenotype of *mir-17~92* mutant mice was similar to the phenotype of conditional *Dicer*$^{-/-}$ mice (Figures 2M–2T),

suggesting that miRNAs generated from the *mir-17~92* cluster are the principal contributors to the silencing of Olig2 expression in p2 progenitors.

The survival of *mir-17~92*$^{-/-}$ embryos until birth provided an opportunity to investigate the consequences of Olig2 expansion into the p2 domain for the generation of neuronal diversity in the ventral spinal cord. Progenitors in p0, p1 and p2 domains give rise to molecularly distinct interneuron populations (Figures 1A and 8) (Briscoe et al., 2000). Consistent with the reduction in p2 progenitors in *mir-17~92*$^{-/-}$ embryoid bodies, Chx10^{on} V2a interneurons were reduced by ~70%, whereas the numbers of Evx1^{on} V0 interneurons and En1^{on} V1 interneurons derived from p0 and p1 progenitors were unaffected (Figures 6F–6J) on day 6 of differentiation. These findings indicate that the decrease in p2 progenitors observed in differentiating cells lacking *mir-17~92* function is not compensated and results in a marked reduction of differentiated V2 interneurons. Finally, we examined the specification of ventral interneurons in *mir-17~92* mutant embryos on E11.5 (Figures 7J–7P). Numbers of both Chx10 expressing V2a and GATA3 expressing V2b interneurons were reduced significantly *in vivo* (Figures 7J, 7K, and 7P). In contrast, the number of the Evx1^{on} (V0) interneurons was similar in the *mir-17~92* mutants and control littermates (Figure 7N and 7O–P). Consistent with the dorsal expansion of Olig2 expressing pMN progenitors, postmitotic Hb9^{on} motor neurons occupied more dorsal regions of the ventral spinal cord in *mir-17~92*$^{-/-}$ embryos at E9.5 (Figure 7G and 7H) and E11.5 (Figure 7L and 7M). Quantification of Hb9 expressing cells in the mutant spinal cord revealed an increase in motor neuron numbers on E9.5 but the difference diminished by E11.5, possibly due to the relative increase in the total motor neuron numbers generated from the endogenous pMN domain or due to the death of supernumerary motor neurons.

Finally, we examined whether the loss of *mir-17~92* cluster affected motor neuron subtype specification. Analysis of the median motor column (MMC) neurons expressing Isl1 and Lhx3 and limb innervating lateral motor column (LMC) neurons expressing FoxP1 at E11.5 brachial spinal cord did not reveal significant defects in motor neuron subtype specification or in motor neuron segregation into appropriate motor columns (Figure S6).

Collectively, these findings provide genetic evidence that the *mir-17~92* cluster is required for efficient suppression of pMN marker Olig2 in p2 progenitors and for the generation of a full complement of V2 spinal interneurons (Figure 8).

DISCUSSION

Cross-repressive interactions are fundamental mechanisms underlying specification of cell identity during embryonic development. Lineage specific repressors restrict cell potential during development by preventing the activation of genetic programs specifying alternative cell fates. Such mechanisms are well documented in the developing spinal cord where progenitor patterning is largely mediated by transcriptional repressors (Briscoe et al., 2000; Lee et al., 2008). Whether additional repressive mechanisms, such as posttranscriptional repression by miRNAs, contribute to the spatial patterning of neural tissue has not been systematically examined, primarily due to the lack of genetic tool that would facilitate tissue specific manipulation of miRNAs in early stages of embryonic development.

To address the role of miRNAs during neural patterning we employed an *in vitro* ES cell based model of dorso-ventral spinal patterning (Wichterle et al., 2002). This system presents several important advantages. First, ES cell derived neural progenitors are highly homogeneous at the time of neural patterning, therefore global deletion of miRNAs or Dicer function will not be confounded by non-autonomous defects in other tissues. Second, ES differentiation is driven with extrinsic patterning signals, thus minimizing potential

patterning phenotypes caused by misspecification of embryonic organizers. Finally, ES cells are amenable to genetic manipulation, thus providing a convenient system to probe the function of miRNAs, their regulators and targets.

To examine the role of miRNAs during spinal cord dorso-ventral patterning, we generated six new ES cell lines in which expression of miRNAs or spinal patterning transcription factors can be regulated with a high temporal resolution. Importantly, once patterning phenotypes were identified, we were able to confirm them *in vivo*, in embryos lacking all or only specific subsets of miRNAs. Together, our studies revealed a previously unappreciated role of miRNAs in the spatial patterning of the developing neural tube. We provide evidence that miRNAs and specifically the *mir-17~92* cluster is required to specify the dorsal limit of motor neuron progenitor domain boundary by silencing Olig2 expression in the adjacent domain harboring progenitors of V2 interneurons. Additional biochemical studies revealed that a passenger miRNA strand - *mir-17-3p* (*mir-17**) is principally responsible for *Olig2* silencing. Four lines of evidence support our conclusions: i) we demonstrate that the loss of miRNAs leads to ectopic expression of Olig2 in the p2 domain; ii) we demonstrate that *Olig2* 3′UTR is a direct target of *mir-17-3p*; iii) we show that *mir-17* is enriched in the p2 domain and its expression is controlled by Olig2/Irx3 cross-repressive loop; and iv) we show that deletion of a gene encoding the *mir-17~92* cluster phenocopies expansion of Olig2 to p2 domain observed in *Dicer* mutants.

mir-17 Carves the p2 Domain from Olig2 Expressing Progenitors

The Nkx6.1^{+} progenitor domain gives rise to three classes of ventral neurons in the developing neural tube: V2 interneurons, motor neurons, and V3 interneurons (Briscoe et al., 2000; Vallstedt et al., 2001). When overexpressed in intermediate spinal cord, Nkx6.1 activates ectopic Olig2 expression and motor neuron formation, suggesting that Nkx6.1 is an activator of Olig2 expression in the context of the ventral spinal cord (Novitch et al., 2001). Consistent with this observation, we show that the majority of progenitors in both p3 and p2 domains transiently express Olig2 (Dessaud et al., 2010; Dessaud et al., 2007). These results suggest that early Olig2^{on} progenitors undergo a refining patterning step during which Olig2 expression is selectively repressed in prospective p3 and p2 interneuron progenitor domains (Figure 8).

The mechanism underlying Olig2 clearance from the p3 domain relies on repressive activity of Nkx2.2 gene, induced in response to a prolonged Shh exposure (Dessaud et al., 2007). Conversely, it has been proposed that Olig2 expression depends on continuous Shh signaling and its clearance from the p2 domain might reflect attenuation of the signaling pathway by the temporal adaptation mechanism (Dessaud et al., 2010). Our study suggests that the clearance of Olig2 from p2 progenitors is an active process involving miRNA-mediated silencing of *Olig2* mRNA (Figure 8). We demonstrate that induced expression of *mir-17* is sufficient to switch the state of the Olig2/Irx3 cross-repressive loop and to convert Olig2^{on}, Irx3^{off} pMNs to Olig2^{off}, Irx3^{on} p2 progenitors. Thus, *mir-17* fulfills a critical function during ventral spinal cord patterning by carving the p2 progenitor domain out of a broad Olig2 expression domain.

Genetic Network Controlling p2/pMN Identity

Disruption of miRNA biogenesis or deletion of the *mir-17~92* locus results in a dorsal shift in the Olig2/Irx3 boundary. Initially we considered whether the observed phenotype might result from altered sensitivity of neuroepithelial cells to Hh signaling, as proposed by Dessaud et al., 2010. This seems unlikely as the expression level of direct targets of Shh signaling (*Gli1*, *Patched* or Nkx2.2) (Vokes et al., 2007) did not exhibit significant differences between control and experimental condition. Moreover we did not detect

changes in the pattern of Shh expression in the conditional *Dicer* null animals or in the position of other progenitor boundaries sensitive to Shh signaling (Nkx2.2, Nkx6.1or Pax7). As an alternative, we considered whether miRNAs might be directly involved in the patterning of the ventral spinal cord, by contributing to cross-repressive interactions defining neural progenitor identity and progenitor domain boundaries. Our results indicate that *mir-17~92* plays a regulatory role in the cross-repressive loop that commits spinal cells to V2 or motor neuron progenitor identity. We provide evidence that *mir-17-3p* can directly silence *Olig2*, leading to the derepression of p2 marker Irx3 in Nkx6.1^{on} cells. Importantly, we also demonstrate that *mir-17* expression is controlled by Olig2/Irx3 cross-repressive loop; ectopic expression of Irx3 in pMN cells induces expression of *mir*-17 while expression of Olig2 in p2 cells represses *mir-17* expression. Interestingly, differentiation of Olig2$^{-/-}$ cells under conditions that exhibit only a modest upregulation of Irx3 resulted in a similarly modest upregulation of *mir-17* expression. Based on these observations we suggest that *mir-17* is induced in neural progenitors by Irx3 and its repression by Olig2 is an indirect result of Irx3 downregulation. What remains to be determined is whether Irx3 exhibits any Olig2 repressive activity that is independent of *mir-17* or whether *mir-17* is an integral component of the cross-repressive loop, similar to *C. elegans*, where miRNAs *lsy-6* and *mir-273* are the principal repressors within a bistable loop that specifies left-right asymmetry of gustatory neurons (Chang et al., 2004; Johnston et al., 2005).

The discovery of miRNA function in dorso-ventral patterning of the developing spinal cord raises the possibility that posttranscriptional silencing might be employed more broadly to control specification of neural progenitors. In this context it is noteworthy that ~60 miRNAs exhibited differential expression levels in spinal progenitors derived under lo and hi[Hh] conditions. Systematic evaluation of individual differentially expressed miRNAs using the inducible ES cell system employed in this study might provide new insights into the mechanisms controlling neural patterning and differentiation. Furthermore, *mir-17* mediated repression of Olig2 might not be limited to the developing spinal cord, as Olig2 is expressed relatively broadly during neural development (Furusho et al., 2006; Shibasaki et al., 2007; Zhou et al., 2001). Besides their role in the patterning of the dorso-ventral axis of the developing neural tube, miRNAs might also be involved either as principal patterning repressors or by acting cooperatively with previously identified transcriptional repressors to define the rostro-caudal progenitor domains and boundaries in the developing CNS. Hox gene expression pattern in the developing axial skeleton and limb bud has been shown to be controlled in part by *mir-196* (Hornstein et al., 2005; McGlinn et al., 2009) and overexpression of *mir-10* in zebrafish embryo is sufficient to repress *Hoxb1* within the developing hindbrain (Woltering and Durston, 2008). Together, these studies raise the possibility that endogenous miRNAs may play a role in rostro-caudal patterning of the developing CNS, and potentially in Hox-mediated specification of spinal motor neuron subtype identity (Dasen et al., 2003; Dasen et al., 2005). We propose that the combined *in vitro/in vivo* approach introduced in this study will be generally applicable to interrogate functions of other miRNAs during spatial and temporal patterning of the developing nervous system.

EXPERIMENTAL PROCEDURES

Mouse ES Cell Culture and differentiation

ES cells were cultured and differentiated as previously described (Wichterle and Peljto, 2008), unless specified otherwise in the text.

Mouse crosses and *in vivo* studies

Olig2$^{Cre/+}$ mice (Dessaud et al., 2007) were crossed to the reporter mice *ROSA26-loxp-STOP-loxp-YFP* mice (Srinivas et al., 2001). Embryos were analyzed at E11.5.

CAGG-CreER mice (Hayashi and McMahon, 2002) were crossed with *Dicer*$^{loxp/loxp}$ (Harfe et al., 2005) to generate *CAGG-CreER*$^{+/-}$*; Dicer*$^{loxp/WT}$ strain. *CAGG-CreER*$^{+/-}$*; Dicer*$^{loxp/WT}$ then mated with *Dicer*$^{loxp/loxp}$ for experimental analysis. Tamoxifen (Sigma, C-8267) was injected intraperitoneally (1.5–2 mg/30g pregnant mice) to activate *CreER* recombination between 5 p.m. and midnight on embryonic day E5.5. Embryos were analyzed at E9.5.

The generation of *mir-17~92*$^{-/-}$ mouse was described in Ventura et al., 2008. Embryos were analyzed at E9.5 and E11.5.

Quantitative real time PCR and TLDA arrays

ES cells or embryoid bodies were harvested for total RNA isolation by mirVana kit (Ambion). For mRNA analysis, 20 ng of total RNA from each sample was reverse transcribed with Superscript III (Invitrogen). One-tenth of the reverse transcription reaction was used for subsequent qRT-PCRs, which were performed in duplicate on an Mx 3000P real time PCR machine (Stratagene) using SYBR Green PCR mix (Stratagene) for each gene of interest and an HPRT or β-actin endogenous control primer probe set for normalization. Each qRT-PCR was performed on at least three different experimental samples.

For miRNA analysis, 20 ng of total RNA was reverse transcribed with a miRNA-specific primer from TaqMan MicroRNA Assays (Applied Biosystems). A ubiquitous small nucleolar RNA, sno202 or sno234, was used as the endogenous control. Each qRT-PCR was performed on at least three different experimental samples.

Rodent TaqMan® Low Density Array (TLDA) version 1 microfluidics cards (Applied Biosystems) were used to assess the miRNA profiles in lo[Hh] and hi[Hh] treated embryoid bodies. The contents of the TLDA card comprised a total of 343 miRNAs. Two different experimental samples from each condition were profiled by ABI Prism 7900HT Sequence Detection System and miRNA levels were normalized to 18S RNA. The array data were analyzed by SDS software (Applied Biosystems) using the RQ = $2.0^{\Delta\Delta Ct}$ method, filtered on flag calls, then analyzed for reproducibly upmodulated and downmodulated profiles by Pavlidis Template Matching and visualized by unsupervised hierarchical clustering within the TM4 analysis package (Saeed et al., 2003).

Immunostaining and antibodies

For the list of antibodies please refer to the Supplemental Experimental Procedures. Images were collected on a Zeiss LSM510 confocal microscope.

miRNA *in situ* hybridization

In situ hybridizations were performed in 15 μm cryosections from E9 to E11 cervical/brachial spinal cord (Silahtaroglu et al., 2007). Sections were fixed in 4% paraformaldehyde and acetylated in acetic anhydride/triethanolamine, followed by washes in PBS. Sections were then pre-hybridized in hybridization solution (50% formamide, 5× SSC, 0.5 mg/mL yeast tRNA, 1× Denhardt's solution) at room tempature, then hybridized with 3′-DIG labeled LNA probes (3 pmol) (LNA miRCURY probe; Exiqon) at 25°C below the predicted T_m value. After post-hybridization washes in 0.2× SSC at 55°C, the *in situ* hybridization signals were detected using the NBT/BCIP (Roche) or Tyramide Signal Amplification system (PerkinElmer) according to the manufacturer's instructions. Slides were mounted in

Aqua-Poly/Mount (Polysciences, Inc) and analyzed with a Zeiss LSM 510 confocal microscope.

Luciferase reporter assay

Wild-type and two mutated versions of *Olig2* 3′ UTR (*mir-17-5p* or *mir-17-3p* binding sites) were cloned into psiCHECK™-2 vector (Promega). 10^5 Hela cells were plated per well (24 well plate) expanded for 16 hours and co-transfected with a mixture of 60 ng of reporter and 2 μg *mir-17* (GeneCopoeia, Inc) plasmids using 1μl Lipofectamine 2000 (Invitrogen). Cells were lysed 24 hours later and processed for luciferase assay using Dual-Luciferase Reporter Assay System (Promega). We measured luciferase activity by 20/20n luminometer (Turner Biosystems).

Supplementary Material

Refer to Web version on PubMed Central for supplementary material.

Acknowledgments

Special thanks to Andrea Ventura (Memorial Sloan-Kettering Cancer Center) for kindly providing *mir-17~92*$^{+/-}$ founder mice and conditional *mir-17~92* floxed ES cells and for the discussion of our results. We thank Ben Novitch (UCLA) for sharing *Olig2-cre* mice, Tom Jessell for reagents and antibodies, and Michael Kyba (University of Minnesota) for providing inducible 2lox-ES cells. We also thank Laskaro Zagoraiou for her help with analysis of V2 interneurons. We would like to thank Fiona Doetsch for critical reading of the manuscript, discussion and comments and Rosalind Bogan for help with manuscript preparation. We would like to acknowledge The NYU Cancer Institute Genomics Facility for expert assistance with microRNA TLDA profiling. E.O.M. was in part supported by Damon Runyon Cancer Research Fund fellowship and G.C.T. was in part funded by NIH training grant T32HD55165. This research was supported by NIH grants NS058502 and NS055923.

References

Bernstein E, Kim SY, Carmell MA, Murchison EP, Alcorn H, Li MZ, Mills AA, Elledge SJ, Anderson KV, Hannon GJ. Dicer is essential for mouse development. Nature genetics. 2003; 35:215–217. [PubMed: 14528307]

Briscoe J, Pierani A, Jessell TM, Ericson J. A homeodomain protein code specifies progenitor cell identity and neuronal fate in the ventral neural tube. Cell. 2000; 101:435–445. [PubMed: 10830170]

Briscoe J, Sussel L, Serup P, Hartigan-O'Connor D, Jessell TM, Rubenstein JL, Ericson J. Homeobox gene Nkx2.2 and specification of neuronal identity by graded Sonic hedgehog signalling. Nature. 1999; 398:622–627. [PubMed: 10217145]

Chang S, Johnston RJ Jr, Frokjaer-Jensen C, Lockery S, Hobert O. MicroRNAs act sequentially and asymmetrically to control chemosensory laterality in the nematode. Nature. 2004; 430:785–789. [PubMed: 15306811]

Chen JA, Chu ST, Amaya E. Maintenance of motor neuron progenitors in Xenopus requires a novel localized cyclin. EMBO Rep. 2007; 8:287–292. [PubMed: 17304238]

Dasen JS, Liu JP, Jessell TM. Motor neuron columnar fate imposed by sequential phases of Hox-c activity. Nature. 2003; 425:926–933. [PubMed: 14586461]

Dasen JS, Tice BC, Brenner-Morton S, Jessell TM. A Hox regulatory network establishes motor neuron pool identity and target-muscle connectivity. Cell. 2005; 123:477–491. [PubMed: 16269338]

Davis TH, Cuellar TL, Koch SM, Barker AJ, Harfe BD, McManus MT, Ullian EM. Conditional loss of Dicer disrupts cellular and tissue morphogenesis in the cortex and hippocampus. J Neurosci. 2008; 28:4322–4330. [PubMed: 18434510]

Dessaud E, McMahon AP, Briscoe J. Pattern formation in the vertebrate neural tube: a sonic hedgehog morphogen-regulated transcriptional network. Development. 2008; 135:2489–2503. [PubMed: 18621990]

Dessaud E, Ribes V, Balaskas N, Yang LL, Pierani A, Kicheva A, Novitch BG, Briscoe J, Sasai N. Dynamic assignment and maintenance of positional identity in the ventral neural tube by the morphogen sonic hedgehog. PLoS Biol. 2010; 8:e1000382. [PubMed: 20532235]

Dessaud E, Yang LL, Hill K, Cox B, Ulloa F, Ribeiro A, Mynett A, Novitch BG, Briscoe J. Interpretation of the sonic hedgehog morphogen gradient by a temporal adaptation mechanism. Nature. 2007; 450:717–720. [PubMed: 18046410]

Fineberg SK, Kosik KS, Davidson BL. MicroRNAs potentiate neural development. Neuron. 2009; 64:303–309. [PubMed: 19914179]

Furusho M, Ono K, Takebayashi H, Masahira N, Kagawa T, Ikeda K, Ikenaka K. Involvement of the Olig2 transcription factor in cholinergic neuron development of the basal forebrain. Dev Biol. 2006; 293:348–357. [PubMed: 16537079]

Georgi SA, Reh TA. Dicer is required for the transition from early to late progenitor state in the developing mouse retina. J Neurosci. 2010; 30:4048–4061. [PubMed: 20237275]

Harfe BD, McManus MT, Mansfield JH, Hornstein E, Tabin CJ. The RNaseIII enzyme Dicer is required for morphogenesis but not patterning of the vertebrate limb. Proceedings of the National Academy of Sciences of the United States of America. 2005; 102:10898–10903. [PubMed: 16040801]

Hayashi S, McMahon AP. Efficient recombination in diverse tissues by a tamoxifen-inducible form of Cre: a tool for temporally regulated gene activation/inactivation in the mouse. Dev Biol. 2002; 244:305–318. [PubMed: 11944939]

He L, Thomson JM, Hemann MT, Hernando-Monge E, Mu D, Goodson S, Powers S, Cordon-Cardo C, Lowe SW, Hannon GJ, et al. A microRNA polycistron as a potential human oncogene. Nature. 2005; 435:828–833. [PubMed: 15944707]

Hornstein E, Mansfield JH, Yekta S, Hu JK, Harfe BD, McManus MT, Baskerville S, Bartel DP, Tabin CJ. The microRNA miR-196 acts upstream of Hoxb8 and Shh in limb development. Nature. 2005; 438:671–674. [PubMed: 16319892]

Jessell TM. Neuronal specification in the spinal cord: inductive signals and transcriptional codes. Nature reviews. 2000; 1:20–29.

Johnston RJ Jr, Chang S, Etchberger JF, Ortiz CO, Hobert O. MicroRNAs acting in a double-negative feedback loop to control a neuronal cell fate decision. Proceedings of the National Academy of Sciences of the United States of America. 2005; 102:12449–12454. [PubMed: 16099833]

Kanellopoulou C, Muljo SA, Kung AL, Ganesan S, Drapkin R, Jenuwein T, Livingston DM, Rajewsky K. Dicer-deficient mouse embryonic stem cells are defective in differentiation and centromeric silencing. Genes & development. 2005; 19:489–501. [PubMed: 15713842]

Lee S, Lee B, Joshi K, Pfaff SL, Lee JW, Lee SK. A regulatory network to segregate the identity of neuronal subtypes. Developmental cell. 2008; 14:877–889. [PubMed: 18539116]

Li Y, Wang F, Lee JA, Gao FB. MicroRNA-9a ensures the precise specification of sensory organ precursors in Drosophila. Genes & development. 2006; 20:2793–2805. [PubMed: 17015424]

Mansfield JH, Harfe BD, Nissen R, Obenauer J, Srineel J, Chaudhuri A, Farzan-Kashani R, Zuker M, Pasquinelli AE, Ruvkun G, et al. MicroRNA-responsive ‘sensor’ transgenes uncover Hox-like and other developmentally regulated patterns of vertebrate microRNA expression. Nature genetics. 2004; 36:1079–1083. [PubMed: 15361871]

McGlinn E, Yekta S, Mansfield JH, Soutschek J, Bartel DP, Tabin CJ. In ovo application of antagomiRs indicates a role for miR-196 in patterning the chick axial skeleton through Hox gene regulation. Proceedings of the National Academy of Sciences of the United States of America. 2009; 106:18610–18615. [PubMed: 19846767]

Mu P, Han YC, Betel D, Yao E, Squatrito M, Ogrodowski P, de Stanchina E, D’Andrea A, Sander C, Ventura A. Genetic dissection of the miR-17~92 cluster of microRNAs in Myc-induced B-cell lymphomas. Genes & development. 2009; 23:2806–2811. [PubMed: 20008931]

Novitch BG, Chen AI, Jessell TM. Coordinate regulation of motor neuron subtype identity and pan-neuronal properties by the bHLH repressor Olig2. Neuron. 2001; 31:773–789. [PubMed: 11567616]

Novitch BG, Wichterle H, Jessell TM, Sockanathan S. A requirement for retinoic acid-mediated transcriptional activation in ventral neural patterning and motor neuron specification. Neuron. 2003; 40:81–95. [PubMed: 14527435]

Okamura K, Phillips MD, Tyler DM, Duan H, Chou YT, Lai EC. The regulatory activity of microRNA* species has substantial influence on microRNA and 3′ UTR evolution. Nat Struct Mol Biol. 2008; 15:354–363. [PubMed: 18376413]

Saeed AI, Sharov V, White J, Li J, Liang W, Bhagabati N, Braisted J, Klapa M, Currier T, Thiagarajan M, et al. TM4: a free, open-source system for microarray data management and analysis. Biotechniques. 2003; 34:374–378. [PubMed: 12613259]

Shibasaki K, Takebayashi H, Ikenaka K, Feng L, Gan L. Expression of the basic helix-loop-factor Olig2 in the developing retina: Olig2 as a new marker for retinal progenitors and late-born cells. Gene Expr Patterns. 2007; 7:57–65. [PubMed: 16815098]

Silahtaroglu AN, Nolting D, Dyrskjot L, Berezikov E, Moller M, Tommerup N, Kauppinen S. Detection of microRNAs in frozen tissue sections by fluorescence in situ hybridization using locked nucleic acid probes and tyramide signal amplification. Nat Protoc. 2007; 2:2520–2528. [PubMed: 17947994]

Srinivas S, Watanabe T, Lin CS, William CM, Tanabe Y, Jessell TM, Costantini F. Cre reporter strains produced by targeted insertion of EYFP and ECFP into the ROSA26 locus. BMC Dev Biol. 2001; 1:4. [PubMed: 11299042]

Stegmeier F, Hu G, Rickles RJ, Hannon GJ, Elledge SJ. A lentiviral microRNA-based system for single-copy polymerase II-regulated RNA interference in mammalian cells. Proceedings of the National Academy of Sciences of the United States of America. 2005; 102:13212–13217. [PubMed: 16141338]

Ting DT, Kyba M, Daley GQ. Inducible transgene expression in mouse stem cells. Methods Mol Med. 2005; 105:23–46. [PubMed: 15492386]

Vallstedt A, Muhr J, Pattyn A, Pierani A, Mendelsohn M, Sander M, Jessell TM, Ericson J. Different levels of repressor activity assign redundant and specific roles to Nkx6 genes in motor neuron and interneuron specification. Neuron. 2001; 31:743–755. [PubMed: 11567614]

Ventura A, Young AG, Winslow MM, Lintault L, Meissner A, Erkeland SJ, Newman J, Bronson RT, Crowley D, Stone JR, et al. Targeted deletion reveals essential and overlapping functions of the miR-17 through 92 family of miRNA clusters. Cell. 2008; 132:875–886. [PubMed: 18329372]

Vokes SA, Ji H, McCuine S, Tenzen T, Giles S, Zhong S, Longabaugh WJ, Davidson EH, Wong WH, McMahon AP. Genomic characterization of Gli-activator targets in sonic hedgehog-mediated neural patterning. Development. 2007; 134:1977–1989. [PubMed: 17442700]

Wang J, Theunissen TW, Orkin SH. Site-directed, virus-free, and inducible RNAi in embryonic stem cells. Proceedings of the National Academy of Sciences of the United States of America. 2007; 104:20850–20855. [PubMed: 18093939]

Wichterle H, Lieberam I, Porter JA, Jessell TM. Directed differentiation of embryonic stem cells into motor neurons. Cell. 2002; 110:385–397. [PubMed: 12176325]

Wichterle, H.; Peljto, M. Curr Protoc Stem Cell Biol. Vol. Chapter 1. 2008. Differentiation of mouse embryonic stem cells to spinal motor neurons; p. 11-19.

Woltering JM, Durston AJ. MiR-10 represses HoxB1a and HoxB3a in zebrafish. PLoS One. 2008; 3:e1396. [PubMed: 18167555]

Wu S, Wu Y, Capecchi MR. Motoneurons and oligodendrocytes are sequentially generated from neural stem cells but do not appear to share common lineage-restricted progenitors in vivo. Development. 2006; 133:581–590. [PubMed: 16407399]

Zhou Q, Anderson DJ. The bHLH transcription factors OLIG2 and OLIG1 couple neuronal and glial subtype specification. Cell. 2002; 109:61–73. [PubMed: 11955447]

Zhou Q, Choi G, Anderson DJ. The bHLH transcription factor Olig2 promotes oligodendrocyte differentiation in collaboration with Nkx2.2. Neuron. 2001; 31:791–807. [PubMed: 11567617]

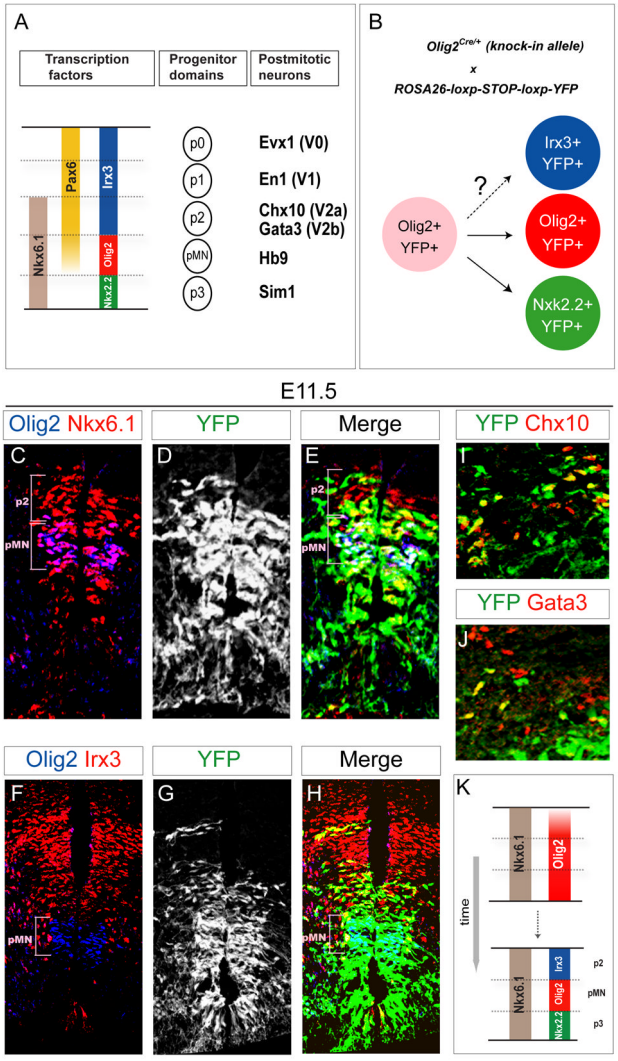

Figure 1. Transient Olig2 Expression in p2 Progenitors

(A) Five cardinal progenitor domains (p0~p2, pMN and p3) are defined in the ventral spinal cord by the combinatorial expression of transcription factors. Each progenitor domain generates different set of ventral spinal interneurons or motor neurons. For more details, see Briscoe et al., 2000; Novitch et al., 2001.

(B) Schematic illustration of Olig2 lineage tracing. Ventral progenitor cells that express Olig2 and all their progeny are indelibly marked by YFP expression in *Olig2$^{Cre/+}$; ROSA26-loxp-STOP-loxp-YFP* embryos.

(C–H) Analysis of Olig2 lineage (YFP^{on} cells) in *Olig2$^{Cre/+}$; ROSA26-loxp-STOP-loxp-YFP* E11.5 spinal cord sections. YFP is expressed in a broad ventral domain that includes p3 progenitors and a subset of p2 progenitors (Olig2^{off}, Irx3^{on} and Nkx6.1^{on}) ventral and dorsal to the pMN (Olig2^{on}) domain.

(I and J) A subset of V2a (Chx10^{on}) and V2b (Gata3^{on}) interneurons derived from p2 domain expresses YFP. For quantification see supplementary Figure S1.

(K) Olig2 is transiently expressed in three ventral spinal progenitor domains. Olig2 expression is selectively down-regulated in p2 and p3 progenitors during spinal cord patterning.

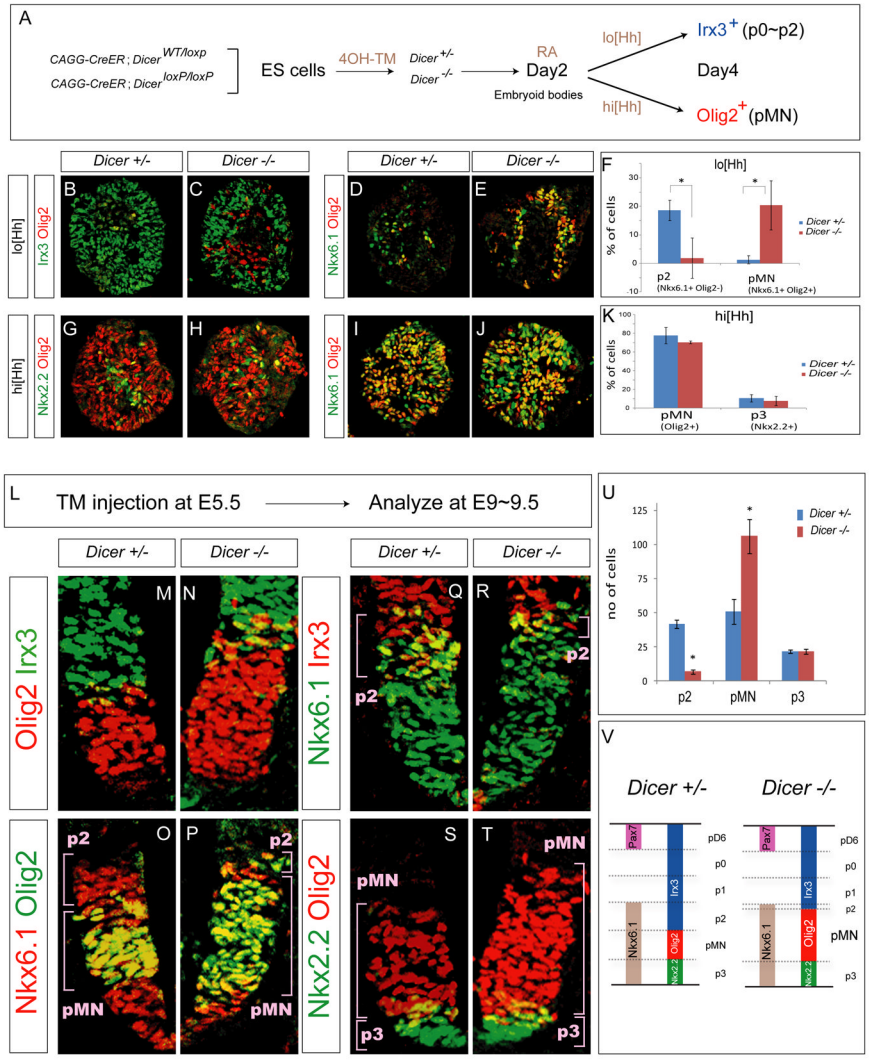

Figure 2. Ectopic Olig2 Expression in the p2 Domain in *Dicer*$^{-/-}$ Embryoid Bodies and Embryos

(A) *CAGG-Cre; Dicer*$^{WT/loxp}$ and *CAGG:Cre; Dicer*$^{loxp/loxp}$ ES cell lines (referred to as *Dicer*$^{+/-}$ and *Dicer*$^{-/-}$ after 4-hydroxytamoxifen (4OH-TM) treatment). ES cells are differentiated with RA (1 μM) and lo[Hh] (5 nM) or hi[Hh] (500 nM) on day 2 and spinal progenitor identities are determined by immunostaining embryoid body sections on day 4.

(B–E) Increase in the fraction of cells expressing pMN identity (Nkx6.1^{on}, Olig2^{on}, Irx3^{off}) and decrease in the number of p2 progenitors (Nkx6.1^{on}, Olig2^{off}, Irx3^{on}) in *Dicer*$^{-/-}$ embryoid bodies under lo[Hh] condition.

(G–K) The pMN (Olig2^{on}) and p3 (Nkx2.2^{on}) progenitors are not affected in *Dicer*$^{-/-}$ embryoid bodies under hi[Hh] condition.

(F and K) Quantification of progenitor cells (percentage of total cells, mean ± SD; n=3 independent experiments) reveals decrease in p2 ($p < 0.01$) and increase in pMN ($p < 0.01$) progenitors in *Dicer*$^{-/-}$ embryoid bodies under lo[Hh] condition, but no change in p3 and pMN fractions under the hi[Hh] conditions.

(L) To study the function of *Dicer* gene *in vivo*, pregnant *Dicer*$^{loxp/loxp}$ mice mated with *CAGG-Cre; Dicer*$^{WT/loxp}$ males were injected with Tamoxifen (TM) on E5.5 and embryos were analyzed for patterning defects on E9.5

(M–T) Dorsal expansion of Olig2 cells is apparent in the *Dicer*$^{-/-}$ E9.5 embryonic spinal cord sections. In contrast, the size of p2 progenitor domain (Nkx6.1^{on}, Olig2^{off}, Irx3^{on}) is diminished. The positions of dorsal boundaries of Nkx6.1 (p2/p1 boundary) or Nkx2.2 (p3/pMN boundary) are not changed.

(U) Quantification of p2 (Nkx6.1^{on}, Irx3^{on}), pMN (Olig2^{on}) and p3 (Nkx2.2^{on}) ventral progenitors (number of positive cells per 15 μm cervical spinal cord hemisection) in control and *Dicer* mutant embryos (mean ± SD, n = 5 embryos), reveals an increase in the number of pMN and decrease of p2 progenitors ($p < 0.01$).

(V) Summary of phenotypes in the ventral neural tube of *Dicer* mutant embryos. Olig2 is repressed in prospective p3 and p2 domains in control spinal cord. Deletion of Dicer function results in expansion of Olig2 expression into the p2 domain resulting in a diminished number of p2 progenitors.

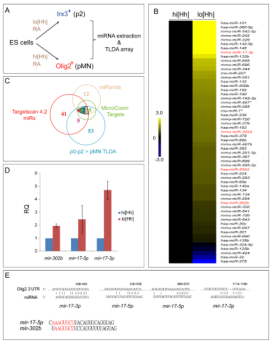

Figure 3. Identification of lo[Hh] Enriched miRNAs Predicted to Target *Olig2*

(A) Small RNAs were isolated from day 4 embryoid bodies differentiated under lo[Hh] or hi[Hh] conditions. Expression levels of miRNAs were analyzed by rodent TaqMan Low Density Arrays (TLDA).

(B and C) A set of miRNAs exhibiting differential expression levels between lo[Hh] and hi[Hh] conditions (n = 2 independent experiments). miRNAs shown in red (B) are the candidates enriched in lo[Hh] progenitors predicted to target to *Olig2* by TargetScan, miRanda and MicroCosm target prediction algorithms (C).

(D) Verification of TLDA data by qPCR in independent differentiation experiments. *mir-17-3p* and *mir-302b* show >2 fold increase in RQ (relative quantity or $2^{-\Delta\Delta}$Ct) in lo[Hh] embryoid bodies when compared to hi[Hh] condition. Data represent three independent experiments (n = 3) performed in triplicate. Error bars indicate SD.

(E) The predicted target sites of *mir-17-3p* and *mir-302b* miRNAs within the 3′UTR of *Olig2*. *mir-17-5p* and *mir-302b* share similar seed sequence (highlighted in red).

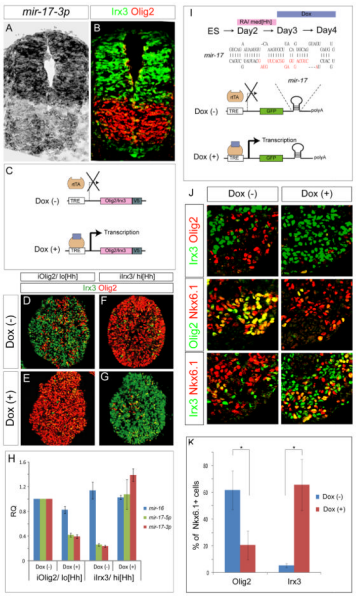

Figure 4. Regulatory Interactions Between *mir-17* and Olig2/Irx3 Cross-repressive Loop

(A) Expression of *mir-17-3p* examined by *in situ* hybridization on E9.5 spinal cord section.

(B) Expression of Irx3, and Olig2 revealed by immunocytochemistry on adjacent spinal cord section.

(C) The design of inducible "Tet-On" ES cell lines expressing Olig2 or Irx3 under the doxycycline (Dox) regulated promoter. In the presence of Dox, the reverse tTA (rtTA) activator is recruited to the TRE (Tetracycline Response Element), thereby initiating the transcription of the downstream gene.

(D–G) Expression of Irx3 is repressed in inducible Olig2 (iOlig2) day 4 embryoid bodies differentiated under lo[Hh] condition and treated with Dox on day 3 (D–E). Conversely, expression of pMN marker Olig2 is extinguished upon the induction of Irx3 (iIrx3) expression by Dox treatment of day 3 embryoid bodies differentiated under hi[Hh] condition (F–G).

(H) The expression levels of *mir-16*, *mir-17-5p*, and *mir-17-3p* were analyzed by qPCR after induction of Olig2 or Irx3 in lo[Hh] or hi[Hh] treated embryoid bodies, respectively. Data were normalized to expression levels in control lo[Hh] embryoid bodies and represent three independent experiments (n = 3) performed in triplicate. Changes in Olig2/Irx3 status of differentiating cells result in corresponding changes in *mir-17-5p* and *mir-17-3p* expression levels.

(I) Generation of Dox inducible *iMir-17* ES cell line in which *mir-17* hairpin is inserted into 3′UTR of GFP. The *mir-17-3p* sequence is marked in red.

(J) Induction of *mir-17* in embryoid bodies differentiated under med[Hh] on day 3 results in a decrease in Olig2 expressing pMN and an increase in Irx3/Nkx6.1 double positive p2 progenitors.

(K) Induction of *mir-17* results in a significant decrease in the fraction of Nkx6.1^{on} cells expressing Olig2 and increase in the fraction of cells expressing Irx3 upon induction of *mir-17* expression ($p < 0.01$, mean ± SD, n = 3 independent experiments).

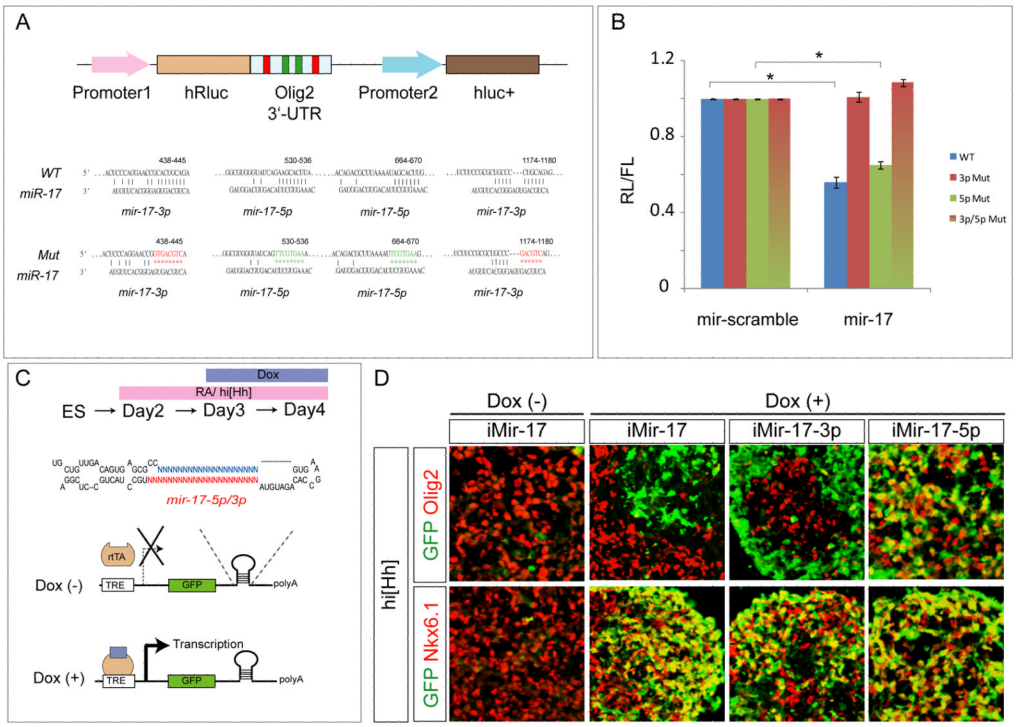

Figure 5. Direct Silencing of Olig2 by *mir-17-3p*

(A) Luciferase reporters were constructed with either a control *Olig2 3′UTR* or the *3′UTR* sequence in which the two potential target sites of *mir-17-3p* were mutated (red), the two potential target sites of *mir-17-5p* were mutated (green), or all four targets sites were mutated (5p/3p Mut).

(B) Co-expression of luciferase construct with *mir-17* in HeLa cells silences reporter carrying intact *mir-17-3p* target sites (WT and 5p-Mut), while *mir-17* fails to silence 3p-Mut and 3p/5p-Mut luciferase constructs (n=3 independent experiments, mean ± SD, $p<0.01$).

(C) Generation of inducible ES cell lines expressing either *mir-17-3p* or *mir-17-5p* (marked in red) as artificial hairpins flanked by *mir-30* backbone (sequence in black) inserted into *GFP 3′ UTR* (Stegmeier et al., 2005). ES cells were differentiated under hi[Hh] (500 nM) condition with or without Dox treatment on day 3 of differentiation.

(D) Expression of Olig2 and Nkx6.1 in embryoid bodies composed of a mixture of control (GFP negative) and inducible (GFP positive) cells. Induction of *mir-17* or *mir-17-3p* on day 3 of differentiation under hi[Hh] condition results in silencing of Olig2 expression, while GFP^{on} cells maintain expression of Nkx6.1. In contrast, induction of *mir-17-5p* has no discernible effect on Olig2 expression.

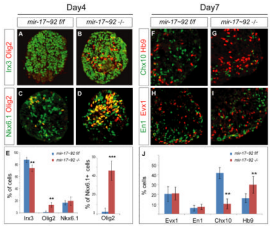

Figure 6. Loss of *mir-17~92* Cluster Results in a Deficit in p2 progenitors and V2 interneurons *in vitro*

(A–E) Expression of Olig2, Irx3 and Nkx6.1 in control and *mir-17~92*$^{-/-}$ embryoid bodies differentiated under lo[Hh] condition. Loss of *mir-17~92* results in an increase in the number of Olig2 positive cells ($p < 0.01$) per section as well as an increase in the fraction of Nkx6.1 positive cells expressing Olig2 ($p<0.001$), mean ± SD, n = 3 independent experiments.

(N–R) Reduction of V2 (Chx10^{on}) interneurons in day 7 *miR-17~92*$^{-/-}$ embryoid bodies cultured under lo[Hh] condition (n = 3, $p < 0.01$). The numbers of V1 (En1^{on}) and V0 (Evx1^{on}) interneurons remain unchanged. Data are quantified as percentage of Chx10, Evx1 and En1 positive cells (mean ± SD; n = 3 independent experiments).

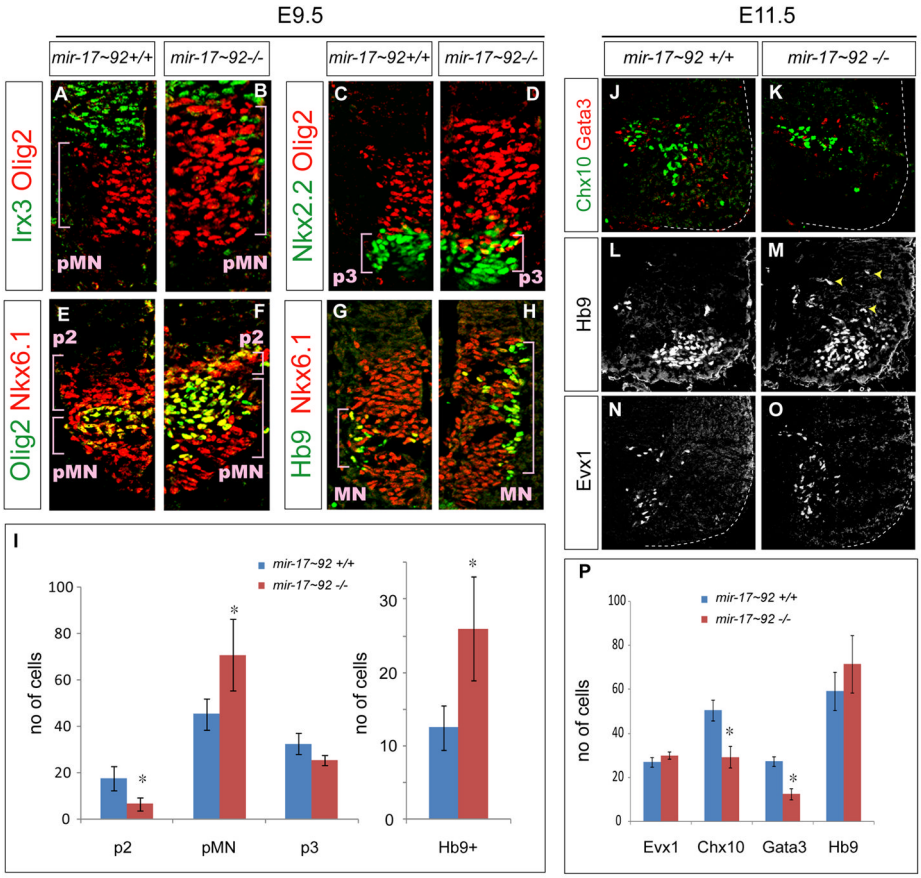

Figure 7. Loss of *mir-17~92* Cluster Results in a Deficit in p2 progenitors and V2 interneurons *in vivo*

(A–H) Dorsal expansion of pMN (Olig2^{on}) progenitor domain is apparent in the *mir-17~92*$^{-/-}$ E9.5 embryonic spinal cord sections. In contrast, the size of p2 progenitor domain (Nkx6.1^{on}, Olig2^{off}, Irx3^{on}) is diminished (E, F). Domains expressing Nkx6.1 or Nkx2.2 are not changed. The location of Hb9^{on} motor neurons is expanded dorsally in the *mir-17~92*$^{-/-}$ embryos (G, H).

(I) Quantification of p2, pMN and p3 ventral progenitors (number of positive cells per 15 μm cervical spinal cord hemisection) in control and *mir-17~92* mutant embryos, mean ± SD reveals a decrease in the number of p2 and an increase in the number of Olig2^{on} pMN progenitors and Hb9^{on} motor neurons ($p < 0.01$; n = 6 embryos).

(J–O) Immunostaining of E11.5 spinal cord sections reveals dorsal shift in the distribution of Hb9^{on} motor neurons (M, arrowheads) and decrease in Chx10^{on} V2a and Gata3^{on} V2b interneurons in *miR-17~92* mutant embryos. In contrast, Evx1^{on} V0 interneurons appear to be unchanged.

(P) Quantification of ventral postmitotic V0, V2a and V2b interneurons, and motor neurons (MNs) (number of positive cells per 15 μm brachial spinal cord hemisection) in control and *mir-17~92* mutant embryos (mean ± SD) reveals a decrease in the number of V2a and V2b interneurons ($p < 0.01$, n = 3 embryos).

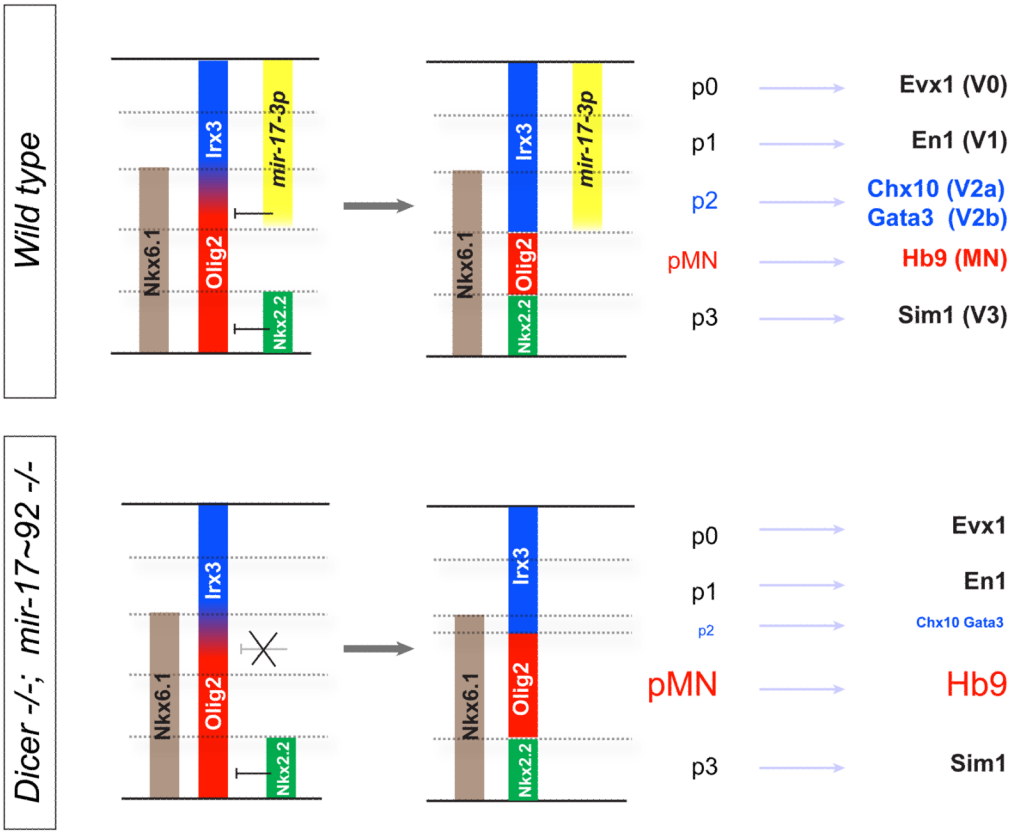

Figure 8. Model of Ventral Spinal Patterning in the Presence and Absence of *mir-17-3p*

A proposed model of dynamic changes in progenitor marker expression in wild type and *Dicer* $^{-/-}$ or *mir-17~92* $^{-/-}$ embryos. In early stages, Nkx6.1 and Olig2 are co-expressed in a broad ventral domain spanning the prospective p3, pMN and part of p2 domains. Subsequently, Nkx2.2 induced by sustained Shh signaling represses Olig2 in the p3 domain (Dessaud et al., 2007) and *mir-17-3p* induced by Irx3 silences Olig2 in the p2 domain, forming the normal p2, pMN, and p3 progenitor domains. In *Dicer* and *mir-17~92* mutant embryos, Olig2 is not efficiently silenced in the prospective p2 domain, resulting in a dorsal shift in the p2/pMN boundary and a deficit in V2 interneurons (Chx10^{on} and Gata3^{on}).